PCCP

Accepted Manuscript

ROYAL SOCIETY OF CHEMISTRY

www.rsc.org/pccp

Cite this: DOI: 10.1039/c0xx00000x

www.rsc.org/xxxxxx

ARTICLE TYPE

Molecular Interactions in the Ionic liquid Emim Acetate and Water Binary Mixtures Probed via NMR Spin Relaxation and Exchange Spectroscopy

Jesse J. Allen, Sage R. Bowser, and Krishnan Damodaran

Received (in XXX, XXX) Xth XXXXXXXXX 20XX, Accepted Xth XXXXXXXXX 20XX
DOI: 10.1039/b000000x

Interactions of ionic liquids (ILs) with water are of great interest for many potential IL applications. 1-Ethyl-3-methylimidazolium (emim) acetate, in particular has shown interesting interactions with water including hydrogen bonding and even chemical exchange. Previous studies have shown unusual behavior of emim acetate when in the presence of 0.43 mol fraction water, and a combination of NMR techniques are used herein to investigate the emim acetate/water system and the unusual behavior at 0.43 mol fraction water. NMR relaxometry techniques are used to describe the effects of water upon the molecular motion and interactions of emim acetate with water. A discontinuity is seen in nuclear relaxation behavior at the concentration of 0.43 mol fraction water, and this is attributed to the formation of a hydrogen bonded network. EXSY measurements are used to determine the exchange rates between the H2 emim proton and water, which show a complex dependence on the concentration of the mixture. The findings support and expand on our previous results which suggested the presence of an extended hydrogen bonding network in the emim acetate/water system at concentrations close to 0.50 mole fraction of H_2O.

1. Introduction

Ionic liquids (ILs), the class of salts with melting points below 100°C, have attracted great attention in recent years as replacements for conventional molecular solvents[1]. Consisting generally of a bulky, organic cation and a smaller organic or inorganic anion, these liquids have great tunability of their properties through the choice of ions and functionalization of these ions[1]. The added complexity of a solvent consisting of both a cation and anion, in addition to the fact that in many cases ILs may be behaving not simply as "innocent" solvents, but instead reacting chemically towards solutes[2], makes important the study of ionic liquids and their mixtures. An understanding of possible solvent-solute interactions is necessary to ensure the proper choice of an ionic liquid as the solvent for a given application, so that favorable solvent-solute interactions can be selected and undesired interactions minimized.

The IL 1-ethyl-3-methylimidzolium acetate (emim acetate, fig 1) has attracted attention as a task-specific solvent, especially for the solvation of carbon dioxide[3] and cellulose[4, 5]. The solvent properties of emim acetate and other 1,3-alkylimidazolium acetate ILs, have been attributed to specific interactions with its solutes, and even reversible chemical reactions[3, 6-9]. As emim acetate is completely miscible with water in all concentrations and is extremely hygroscopic[10], water will be present in all samples except those which are highly purified and handled with rigorously water-free techniques. Thus, understanding the interactions between emim acetate and water is valuable not only from the perspective of fundamental understanding of emim acetate/water mixtures themselves, but also because these same interactions will be present in any practical utilization of this IL.

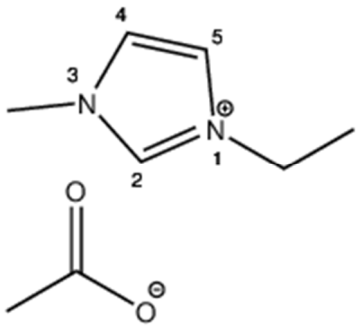

Fig.1 Structure for emim acetate with numbering of imidazolium ring.

A number of studies of emim acetate/ water mixtures have already been carried out.[11-13] Water has been shown to affect the solvent properties of emim acetate, even in low weight fractions.[14] The macroscopic properties of binary emim-acetate/water mixtures have previously been shown to deviate from ideal mixing behavior,[11] and a previous study has shown an extremely concentration-dependent deviation in the self-diffusion behavior for 0.44 mole fraction water mixtures.[15] Our motivation for the studies described in this work was to continue the study the non-linear concentration dependence of the behavior of emim acetate/water mixtures on the microscopic level. We report here

two nuclear magnetic resonance (NMR) investigations of the microscopic interactions of emim acetate and water. Concentrations ranging from 0.05-0.79 mole fraction water are investigated, with particular focus on one sample at a concentration of 0.43 mole fraction water which shows aberrant behavior.

In the first part of the work, we employ NMR relaxometry measurements to determine the nuclear magnetic relaxation properties of emim acetate/water mixtures. The relaxation times of nuclear spins are sensitive to both intra- and intermolecular relaxation mechanisms.[16] High-resolution NMR relaxometry measurements can determine the spin-lattice (T_1) and spin-spin (T_2) relaxation rates of each nucleus in the system, creating a relaxation "map" of the molecule.[17] When two NMR-active nuclei form a bond, the rate of rotation of the bond vector, or rotational correlation time (τ_c) can be determined from the spin-lattice relaxation times (T_1) of the nuclei and Nuclear Overhauser Enhancement (NOE) factor between the nuclei.[18-23] We report and discuss the concentration-dependence of the relaxation times and rotational correlation times, which exhibit a discontinuity at 0.43 mole fraction water.

In the second part of this work, we measure a specific chemical interaction between emim acetate and water, proton exchange, using 2D Exchange Spectroscopy (EXSY) NMR. EXSY is a technique which measures the transfer of magnetization due to chemical exchange, allowing determination of the exchange rate.[24] The weak carbon acidity of 1,3-substituted imidazolium compounds is well documented,[25-29] and the concentration dependence of the rate of the imidazolium-water proton exchange has been used previously to probe the water-anion interactions in an IL.[30] As the pK_b of acetate is relatively low, acid-base equilibrium is likely to play a significant role in this interaction. We show that as expected, the proton exchange rate is much greater in emim-acetate water mixtures than in previously studied mixtures of water and other imidazolium ILs with less basic anions, and that the concentration dependence of the exchange rate is complex.

2. Experimental

Emim acetate was purchased from Sigma Aldrich and used as received. NMR samples were prepared in medium-walled NMR tubes. A sealed capillary containing DMSO-d6 was added to each NMR sample to allow for calibration of chemical shift values. Shortly after preparation, each NMR tube was sealed with a flame to prevent concentration change due to evaporation of the sample or absorption of atmospheric water. Six samples, containing mole fractions of water, 0.05, 0.24, 0.40, 0.43, 0.62, and 0.79 were prepared. To avoid errors in concentration caused by possible evaporation during the sealing process, the mole fractions of emim acetate and water in the samples were determined by integration of the ^{1}H proton spectra under quantitative conditions.

^{1}H and EXSY NMR experiments were performed on a Bruker Avance III 600MHz NMR spectrometer operating at a 1H frequency of 600.71 MHz, equipped with an inverse probe. Sample temperature was controlled by the incorporated heating element of the probe and a flow of dry air at 535 l/h from an external refrigeration unit. The temperature readings from the internal probe thermocouple were calibrated using the difference in CH_3 and OH chemical shifts of a sample of 80% ethylene glycol in DMSO-d6. The temperature was equilibrated for at least 30 minutes prior to any data acquisition. Shimming was performed on the ^{1}H signal of greatest intensity using the 3D Topshim gradient shimming algorithm incorporated in Bruker Topspin (Bruker Biospin, Billerica, Massachusetts, USA) software. The experiments were carried out without deuterium field lock due to the poor signal-to-noise ratio of the lock signal.

The 2D EXSY spectra were acquired using the non-gradient selected, phase-sensitive program noesyph included in Bruker Topspin. A total of 2048 (f2) x 64 (f1) points were acquired for each spectra, with 16 scans being acquired for each experiment. A relaxation delay of 6s was used. Data were acquired for each concentration using mixing times of 0ms and 100ms at 60°C, 70°C, and 80°C. The 100ms spectrum for each temperature point for each concentration was repeated three times. The spectra were phase-corrected manually in the f2 dimension and automatic baseline correction was applied to both the f2 and f1 dimensions, and the volumes of the H2 and H_2O diagonal and cross-peaks were integrated. All processing operations were carried out using the Bruker Topspin software package (Bruker Biospin, Billerica, Massachusetts, USA).

NMR relaxometry measurements were performed using a Bruker Avance III 600MHz NMR spectrometer operating at a 1H frequency of 600.71 MHz. The employed probe was a direct-observe BBFO plus (broadband including fluorine) probe. Relaxation measurements were carried out with relaxation delays at least five times T_1, and the instrument was carefully tuned, shimmed, and the 90 degree pulse calibrated before each measurement. T_1 relaxation measurements were done with an inversion recovery pulse sequence. ^{13}C T_1 relaxation measurements were done with ^{1}H decoupling throughout the relaxation time, to prevent any cross relaxation effects.[18, 19, 22] T_2 measurements were made using a CPMG pulse sequence.

Measured ^{13}C NOE enhancement factors were calculated as in equation 1, where $\eta_{measured}$ is the NOE enhancement factor, N_H is the number of protons directly bound to the carbon atom being measured, I_{PG} is the intensity of the peak resulting from full NOE enhancement by polarization transfer from protons in a power gated experiment, and I_{IG} is the intensity of the peak resulting from an inverse gated experiment, experiencing no NOE enhancement by proton polarization transfer.[16] Pulse sequences used are included as text files in the supporting information.

$$\eta_{measured} = \left(\frac{I_{PG}}{I_{IG}} - 1\right)/N_H \quad (1)$$

Calculations of rotational correlation times were performed by the method developed by Carper et al.[18-20, 22] and are included in the supplemental information. Iterative calculations were performed using the Goalseek™ function of Excel®.

3. Results and Discussion

3.1 NMR Relaxometry Measurements

Relaxation measurements of emim acetate were used to characterize segmental motions and molecular interactions. Spin-lattice relaxation times (T_1) and spin-spin relaxation times (T_2) were measured using NMR spectroscopy. These relaxation times

are known to be sensitive to several factors such as electronic effects, mobility, and intermolecular interactions.[31-34]

Magnetic field fluctuations are the major cause of nuclear spin relaxation. Localized association of nuclear spins can cause increased relaxation rates; in this way relaxation measurements and NOE factors can be used as evidence of localized interactions.[31-34] Rotational correlation times are calculated from relaxation measurements and NOE enhancement measurements, and are used to represent motions of molecule segments. Segmental motion can be very important for interactions with small molecules and for understanding interactions related to the physical properties of ionic liquids.

NMR has previously been used to characterize the molecular interactions of emim acetate with water by Hall, et al. with a focus upon high concentrations of water. These studies, however, measured the relaxation of the entire molecule rather than relaxation of the individual nuclei present.[11] Previous diffusion and computational studies have shown the formation of a hydrogen bonded network in emim acetate/water mixtures,[15] and the formation of this hydrogen bonded network should have significant effects upon nucleus spin relaxation.

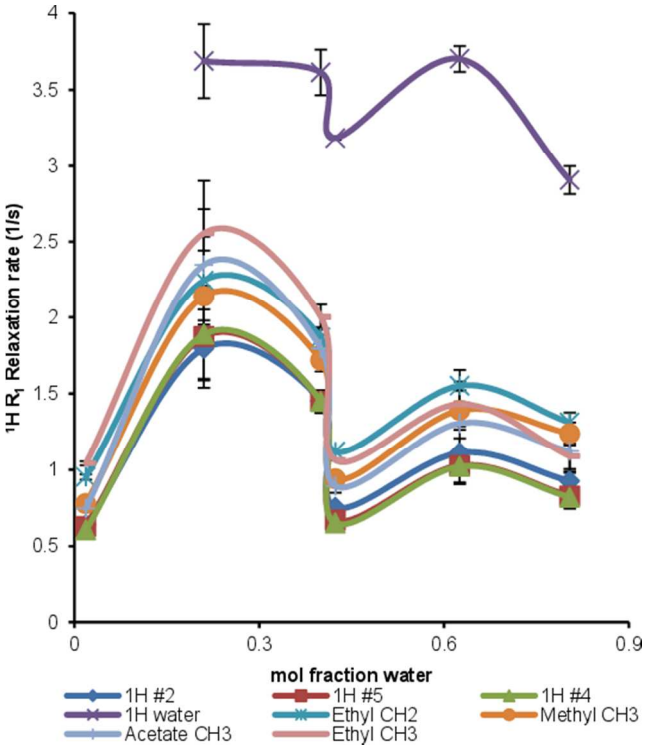

Fig. 2 ^{1}H R_1 spin-lattice relaxation rates as a function of emim acetate to water molar ratio show a peak in relaxation rates at 0.24 mole fraction water. This is attributed to the competing effects of changes in viscosity and the propensity for water to cause dipolar relaxation with neighboring molecules. The graph including is discontinuous at 0.43 mole fraction water. This discontinuity is taken to represent the concentration where a network of hydrogen bonds is forming.

The main effects acting upon relaxation rates due to the addition of water are:

1. Increasing water decreases viscosity, increasing molecular motion.
2. Increasing water increases available dipolar relaxation pathways.
3. Water increases the availability of hydrogen bonding, which can slow rotation.

Proton spin-lattice relaxation rates (R_1) are plotted against molar concentration of emim acetate in fig 2. The addition of water causes large increases in emim acetate molecular motion, as water is much less viscous than emim acetate. Increased motion causes faster molecular tumbling, which slows the spin-lattice relaxation rate. At the same time, however, the addition of water to the ionic liquid emim acetate enables more dipolar relaxation with nearby water molecules. This dipolar relaxation through water molecules causes faster spin-lattice relaxation, and the two competing effects result in a peak at 0.24 mole fraction water in fig. 2. The very fast relaxation rate of water in the sample is expected due to the prevalence of hydrogen bonds occurring with water. The deviation from expected behavior in 0.43 mole fraction sample is taken as evidence of an extended hydrogen bonded network.[15]

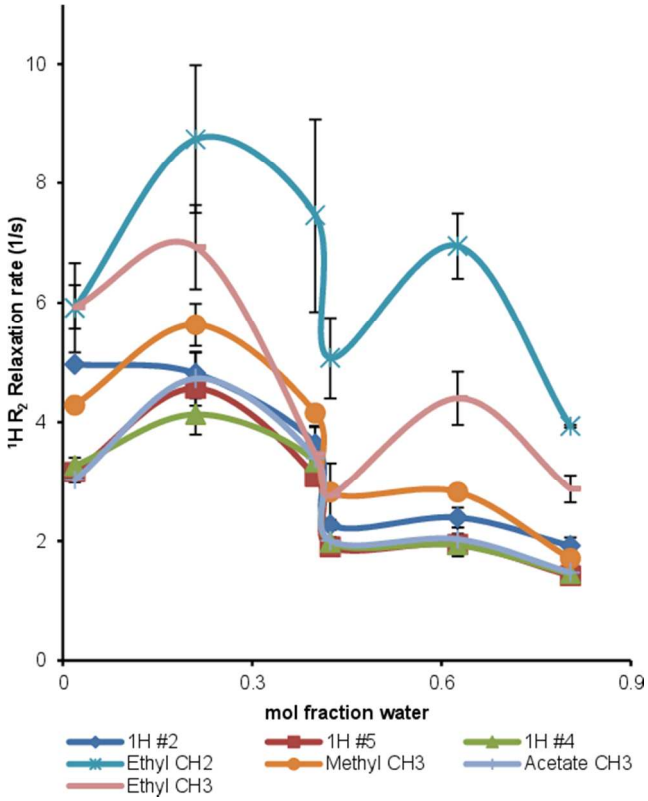

Fig. 3 ^{1}H R_2 spin-spin relaxation rates as a function of emim acetate to water molar ratio show a peak in relaxation rates at 0.24 mole fraction water. This is attributed to the competing effects of changes in viscosity and the propensity for water to cause dipolar relaxation with neighboring molecules. A dip in the graph is clearly seen with the 0.43 mole fraction water sample, showing the change in dynamics that occurs at this concentration.

Spin-spin relaxation of ^{1}H nuclei (fig. 3) shows similar trends to the spin-lattice relaxation of ^{1}H nuclei. The CH_2 of the ethyl group shows fast relaxation, an order of magnitude greater than that expected for the group. The fast spin-spin relaxation of the ethyl group is surprising and may indicate some kind of interaction, though it is premature to suggest what kind of

interaction may be occurring at that site. Water, as expected, shows very fast relaxation due to the prevalence of hydrogen bonds (See fig S2 of supplementary data).

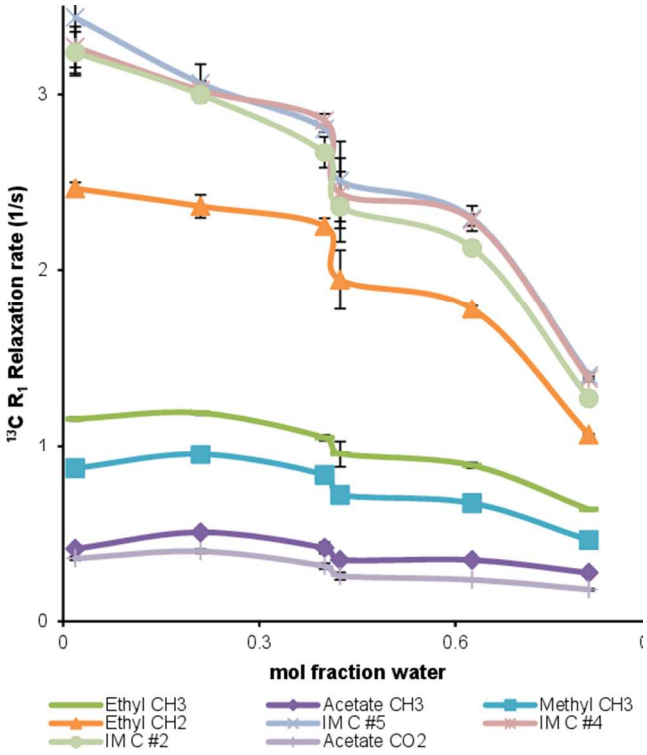

Fig. 4 ^{13}C R$_1$ spin-spin relaxation rate as a function of emim acetate to water molar ratio is shown. The graph shows a significant dip at the sample with 0.43 mole fraction water. As carbon relaxation is dominated by through-bond dipolar relaxation with protons, a consistent peak is not seen for maximal relaxation rate of carbon nuclei.

Figs 4 and 5 show that ^{13}C spin-lattice and spin-spin relaxation rates increase as water concentration decreases. The increase in relaxation rates is due to the decreased level of molecular motion when less water is present. Relaxation rates for CH_2 and CH groups show increased dependence upon water concentration when compared with CH_3 groups and the anion due to hindered rotational motion. CH and CH_2 groups are more dependent upon molecular tumbling and rotation of the whole molecule when compared with CH_3 groups. CH_3 groups also show much slower relaxation due to their fast rotational motion. Spin-spin relaxation (fig 5) of the carboxylic group does not seem to be correlated with water concentration, which is likely due to the lack of directly bound hydrogen nuclei, decreasing the level of dipolar relaxation. Carboxylate group relaxation is also very slow, which is due to the combination of it lacking directly bound protons for dipolar relaxation, and the very fast molecular tumbling experienced by being a small molecule.

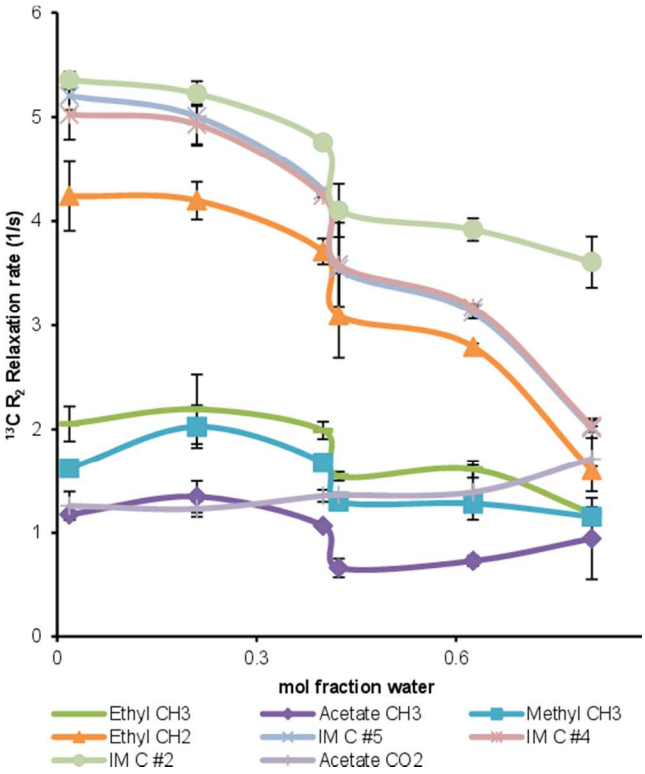

Fig. 5 ^{13}C R$_2$ spin-spin relaxation rates as a function of emim acetate to water molar ratio show no consistent peak in relaxation rates. This is attributed to the effect of dipolar relaxation with neighboring molecules being the dominant relaxation pathway. The discontinuity in the graph occurs at 0.43 mole fraction water, where it is postulated that a significant increase in hydrogen bonding is occurring.

3.2 Segmental Dynamics

Relaxation of spin ½ nuclei is highly dependent upon motion. For carbon atoms directly bound to hydrogen atoms, careful design of relaxation experiments allows for measurement of T_1 relaxation times which almost exclusively represent relaxation through the dipolar relaxation mechanism.[18-20, 22] The dipolar coupling constant can then be calculated using equation 2:

$$D_{ij} = \frac{\mu_0}{4\pi}\gamma_C\gamma_H\frac{\hbar}{2\pi}r_{ij}^{-3} \qquad (2)$$

where D_{ij} is the dipolar coupling constant, μ_0 is the permeability of a vacuum, γ_C is the gyromagnetic ratio of carbon, γ_H is the gyromagnetic ratio of hydrogen, $\hbar$ is the reduced Planck's constant, and r_{ij} is the length of the bond between carbon i and proton j (estimated by computational methods). Dipolar relaxation can be related to both the rotation rate of the vector between the spin systems (rotational correlation time, τ_C) and the NOE factor by equation 3:

$$\tau_C = \frac{10}{T_{1N_H}(2\pi D_{ij})^2}\left(\frac{1}{1+(\omega_C-\omega_H)^2\tau_C^2}\frac{3}{1+\omega_C^2\tau_C^2}\frac{6}{1+(\omega_C+\omega_H)^2\tau_C^2}\right)^{-1} \qquad (3)$$

where τ_C represents the rotational correlation time (The time it takes for the vector defined by the C-H bond to rotate by one radian), N_H is the number of directly bound protons, and ω_X and ω_H are the Larmor frequencies of carbon and hydrogen,

respectively. τ_C, found iteratively from inserting equation 2 into equation 3 can be corrected using the measured and theoretical maximum NOE factors ($\eta_{measured}$ and η_{max}, respectively) by equations 4 and 5.[20]

$$\eta_{max} = N_H\left(\frac{T_1^{DD}}{20}\frac{\gamma_H}{\gamma_C}\left(2\pi D_{ij}\right)^2\left(\frac{12\tau_C}{1+(\omega_C+\omega_H)^2\tau_C^2} - \frac{2\tau_C}{1+(\omega_C-\omega_H)^2\tau_C^2}\right)\right) \quad (4)$$

$$R_1^{Dipolar} = \left(\frac{\eta_{measured}}{\eta_{max}}\right)/T_1^{measured} \quad (5)$$

An example of the rotational correlation time calculation can be found in table S1; values of constants are included as table S2.

Rotational correlation times have been calculated for all C-H bonds which have unambiguously assigned ^{13}C resonances, except those involving the bond between a ring carbon and a proton.[18-20, 22, 35] These atoms are labeled as in fig 1. The C-H bonds at positions 2, 4, and 5 were not calculated because of likely hydrogen bonding occurring at these sites, which invalidates these calculations by providing a significant contribution to dipolar relaxation. The CH_3 from the methyl group and the acetate group show expected tendencies, with very fast rotational correlation times (10-20 ps). The CH_3 from the ethyl group, however; shows significant rotational slowing to correlation times in the 40-70 ps range. This rotational slowing is also seen in the CH_2 from the ethyl group, with correlation times at ~120-155 ps. The rotational slowing of the CH_2 portion of the ethyl group can easily be explained by its attachment to the imidazolium ring, though the significant rotational slowing of the CH_3 portion of the ethyl group is less clear. The rotational correlation times for the imidazolium ring C-H bonds were not calculated, as the bond lengths are known to change due to hydrogen bonding with water, invalidating the calculations.[18-20, 22]

Table 1 Rotational correlation times (τ_c) for the molecule emim acetate[a]

Mole fraction Water	Ethyl CH_3	Acetate CH_3	Methyl CH_3	Ethyl CH_2
0.052	71	14	16	134
0.24	61	16	19	145
0.40	67	15	19	153
0.43	52	12	15	130
0.62	62	14	21	156
0.79	39	11	18	122

[a] Aromatic C-H bonds were not considered viable for τ_c calculations, as the potential for hydrogen bonding invalidates the calculation.

3.3 Determination of Proton Exchange Rates by EXSY

The acidity of the H2 proton of the 1,3 –substituted imidazolium cation has been widely studied,[26, 29] with reported pKa values ranging from 21.2 for the 1,3-bis-((S)-1-phenylethyl)benzimidazolium cation in aqueous solution[26] to 24 for 1,3-diisopropyl-4,5-dimethylimidazolium in DMSO-d_6.[29] The reactivity of 1,3-substituted imidazolium cations towards water has also been studied in dilute aqueous solutions of imidazolium salts.[26, 27] However, to the best of our knowledge, only two reports of the proton exchange rates in concentrated IL/water mixtures have been published.[30, 36]

The rates of proton exchange between the H2 proton of the emim cation and water were determined using 2D EXSY. The 2D-EXSY spectra showed no strong cross peaks other than those between water and the H2-proton of the imidazolium cation, indicating that this is the only exchange process occurring on the slow to medium NMR timescale for the emim acetate/water mixtures studied. After a preliminary study at temperatures between 30°C and 100°C, the temperature range between 60°C and 80°C was chosen for extensive study, as at these temperatures the exchange cross peaks were intense enough to give reliable integrations, while being well below the boiling point of the lower-boiling component of the mixture, water.

The rate constants of magnetization transfer between the two sites were determined from the peak volumes of the 2D EXSY spectra. Representative 1D ^1H spectra for each sample and temperature can be found in figures S3-S8 along with representative EXSY spectra in figures S9-S26. Values of the EXSY peak volumes can be found in tables S3-S8.

Evaluation of the rate constants was carried out by full matrix analysis with the EXSYCalc software package (Mestrelab Resesarch, Santiago de Compostela, Spain), using the mathematical treatment for a two-site exchange with unequally populated sites. Briefly, this method is based on the fact that intensities of the cross and diagonal peaks of exchanging sites in a 2D EXSY spectrum are related to the rate of magnetization exchange between the sites and to the experimental mixing time. By obtaining the initial intensities of the diagonal peaks at zero mixing time and the intensities of the diagonal and cross peaks after a short mixing time (on the order of hundreds of milliseconds), the rate of magnetization transfer between the two sites can be calculated. A full mathematical description of this analysis method has been published by Macura et al.[37] The forward and reverse rate constants, denoted as k_{AB} and k_{BA}, respectively, of the pseudo-first-order exchange reaction were defined according to fig 6 below.

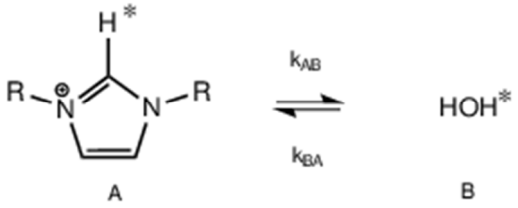

Fig. 6 Pseudo-first order reaction of magnetization transfer measured by 2D-EXSY

The rates of the proton exchange reaction can be calculated from the pseudo-first-order rate constants of magnetization transfer by the relationships given in equations 6 and 7. The factor of two in equation 7 represents the two exchangeable protons of the water molecule. The calculated exchange rates for each temperature and concentration studied are summarized in table 2.

$$v_{AB} = k_{AB}[emim]^+ \quad (6)$$

$$v_{BA} = 2k_{BA}[H_2O] \quad (7)$$

For nearly all mole fractions and temperatures, the forward and reverse rates of the exchange are equal within experimental error,

as would be expected for a two site exchange. The exceptions are the exchange rates of the 0.05 mole fraction water sample at 60°C and 80°C; however, these discrepancies can be attributed to overlap between resonances of water and the resonances of the ^{13}C satellites of the H4 and H5 protons at these temperatures (see figures S9-S11).

The rates observed for this system are considerably faster than the rates observed for other concentrated IL/water mixtures reported in the literature. For the system 1-butyl-3-methylimidazolium chloride/water, the initial rate of H/D isotope exchange between the H2 proton and water at 50°C was lower than 5E-05 M/s for

Table 2 Exchange rates of the H2 and H_2O protons of emim acetate and water at different temperatures

	60°C		70°C		80°C	
Mole Fraction H_2O	ν_{AB} $(\chi s^{-1})^a$	ν_{BA} $(\chi s^{-1})^a$	ν_{AB} $(\chi s^{-1})^a$	ν_{BA} $(\chi s^{-1})^a$	ν_{AB} $(\chi s^{-1})^a$	ν_{BA} $(\chi s^{-1})^a$
0.052	0.06 ± .03	0.15±.08	0.22±.01	0.22±.03	0.37±.02	0.67±.14
0.24	0.49±.02	0.51±.03	1.18±0.4	1.22±.07	2.64±.06	2.71±.12
0.40	0.37±.02	0.37±.03	0.96±.05	0.95±.04	2.15±.06	2.15±.09
0.43	0.67±.03	0.66±.03	1.62±.07	1.55±.08	3.64±.21	3.40±.21
0.62	0.31±.05	0.29±.08	0.81±.13	0.74±.22	1.95±.25	1.80±.46
0.79	0.16±.02	0.12±.02	0.39±.06	0.32±f.05	0.98±.07	0.89±.11

[a] Units of the exchange rate are given in mole fraction per second (χs^{-1}).

samples in the concentration range reported for the current system.[30] Ohta et al. performed a similar H/D isotope exchange experiment using 1-butyl-3-methylimidazolium tetrafluoroborate/water mixtures[36]; although unfortunately rate data was not reported, from fig 4 of that reference, the exchange rate at about 0.45 mole fraction water can be estimated as approximately 9.6E-05 mole fraction/s at 75C.[36]

Fig. 7 Assumed second-order scheme for the analysis of the exchange reaction

The observed rate constants for the exchange for each concentration were then calculated according to the second-order reaction scheme presented in fig 7 and equation 8 below. Following the approach described by Yasaka and coworkers for the 1-butyl-3-methylimidazolium chloride/water system,[30] the constant k_{obs} was plotted using both the "forward" and "reverse" rate constants k_{AB} and k_{BA}; plots of k_{obs} at each temperature and concentration measured are shown in fig 8 below.

For an ideal bimolecular exchange reaction, occurring by a concerted mechanism with the activity of both reactants equal to 1, the exchange rate k_{obs} would be constant for all concentrations. Relative deviations of the apparent second-order rate constant from this ideal behavior indicate deviation of the exchange behavior from the ideal, either due to the reaction proceeding through a mechanism other than the proposed rate law, or interactions within the solution inhibiting the activity of one or both of the reactants, or a combination of both factors.

$$\nu_{ex} = k_{obs}[emim]^+[H_2O] \quad (8)$$

It is clear from the non-constant values of k_{obs} that the rate of exchange is not proportional to the product of $[emim]^+[H_2O]$, and thus that the mechanism of proton exchange between emim and water cannot be approximated through a concerted bimolecular exchange mechanism. It is also clear that the mechanism of proton exchange in the emim acetate/water system is quite different than that of the bmim Cl system studied by Yasaka, in which the exchange rate was seen to increase linearly once a critical concentration of water was present; this behavior was explained through deactivation of water at low concentrations through strong hydrogen bonding with the chloride anion[30]. While hydrogen bonding deactivation, either between the acetate and water, or between acetate and the H2 proton of the cation, could account for the reduced exchange rate of the 0.05 mole fraction H_2O sample compared to that of the 0.20 mole fraction H_2O sample, it does not explain the decrease in rate constant with increasing water concentration which occurs at water concentrations greater than 0.43 mole fraction.

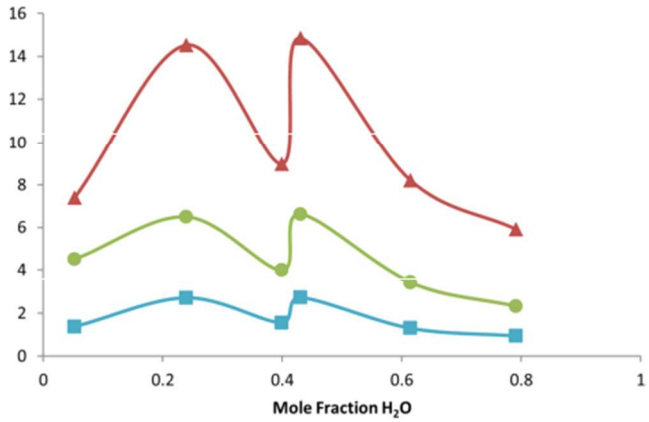

Fig. 8 Plot of apparent second-order rate constant k_{obs} vs. mole fraction of H_2O for the samples studied, at ■ 60°C, ● 70°C, ▲ 80°C. Only data calculated from ν_{AB} are shown. Error bars are within the diameter of the markers. Lines are included as guides for the eye.

As neither a concerted bimolecular exchange reaction, nor deactivation of water by anion-water hydrogen bonds, are sufficient explanation for the deviation of the exchange rates, an alternative explanation must be sought. Given the great similarity

of the emim cation to the bmim cation studied previously, the difference in cation effects between the two should be negligible, and thus the role of the anion should be considered. The proton exchange behavior of the imidazolium cation has been previously reported as a base-catalyzed solvent exchange through the Eigen mechanism pictured in fig 9.[26]

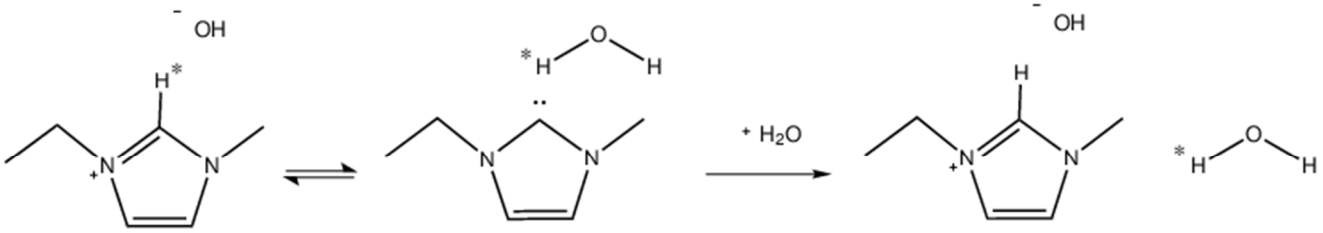

Fig. 9 Proposed base-catalyzed proton exchange reaction with the hydroxide ion as the base. Catalysis by acetate is also possible, followed by rapid proton transfer to water, to give the same overall reaction scheme observed by EXSY.

Emim acetate/water mixtures have been reported to be quite basic, with pH decreasing from a maximum of 14.2 in pure emim acetate, to 12.5 in 10% (w/w) (corresponding to a roughly 1:1 emim acetate:H_2O mole ratio) to 10.9 at 25% w/w H_2O (corresponding to a ~0.70 mole fraction H_2O solution).[13] Additionally, in an exchange study of 1-butyl-3-methylimidazolium tetrafluoroborate/D_2O system, Ohta and coworkers found that at certain mole ratios the H/D proton exchange was strongly inhibited by the presence of hydrofluoric acid, formed as a product of hydrolysis of the anion , but proceeded to equilibrium within five minutes after the solution pH was increased to 11-12 using NaOD.[36] The great increase in the rate of the proton exchange reaction of emim acetate as compared to the exchange rates observed for imidazolium ILs with neutral or acidic anions, as well as the decrease of the observed rate constant with increasing water content of the emim acetate/water mixtures, is therefore tentatively attributed to the extremely basic environment.

A second point worthy of discussion is the large discrepancy between the exchange rates of the 0.40 and 0.43 mole fraction H_2O samples. The aberrant relaxation behavior reported earlier in this work, as well as the previous report of hydrogen bond formation, suggest that there is a fundamental change in the solution structure at this concentration, which may enhance the exchange rate by increasing the concentration or activity of basic species in the solution. However, on the basis of the present data, the alternative possibility of deactivation of the exchange at 0.40 mole fraction H_2O cannot be eliminated.

A quantitative analysis of the effects of the concentration of basic species is not possible from the NMR data. Separate resonances belonging to the hydroxide ion or the carbene conjugate base of emim intermediate predicted by the Eigen mechanism were not observed. However, this does not rule out the presence of these species in the solution, as fast exchange on the NMR timescale with water and the emim cation respectively would result in averaged signals. Nor was any carboxylic acid signal observed from acetic acid, a species whose formation in emim acetate and its mixtures with water has been suggested[38] and which must be present in some concentration if base-catalysis of the exchange reaction is occurring; this can also be attributed to fast exchange and a low equilibrium population.

4. Conclusions

A discontinuity in both NMR relaxation times and NMR exchange rates was seen in the emim acetate/water system at a concentration of 0.43 mole fraction H_2O, consistent with a previous report of enhanced hydrogen bonding at this concentration. NMR relaxometry studies showed concentration dependent trends which were discontinuous at this concentration for all measured carbon and hydrogen nuclei. Exchange spectroscopy also showed discontinuous behavior at this concentration; with a large increase in exchange rates. This strongly supports the findings of Shi, et al. by computational and NMR diffusion measurements[15].

Relaxation measurements showed the competing effects of viscosity and increased availability of protons for dipolar relaxation when looking at different water concentrations in emim acetate. Trends showed a relaxation rate maximum for protons at 0.20 mole fraction water, where water is providing additional protons for dipolar relaxation, but where the solution is also still viscous enough to inhibit molecular motion. ^{13}C relaxation rates are more dependent upon through bond dipolar relaxation, and so did not show the competing effect of increasing relaxation rate from increased available protons. Instead, ^{13}C relaxation rates increased with decreasing water concentration.

Rotational correlation times were calculated for all non-aromatic C-H bonds. These correlation times were used to give indications of segmental motion of emim. The CH_3 groups showed expected fast rotation with the exception of the CH_3 of the ethyl group. It is yet unexplained, but both the CH_2 and CH_3 of the ethyl group showed hindered rotation, which was also evidenced by fast nuclear spin relaxation.

The rate of proton exchange between the H2 position of the imidazolium cation and water has been determined for emim acetate/water mixtures ranging between 0.05-0.79 mole fraction water. The rate of the exchange is found to be much greater than reported for 1,3-alkylimidazolium-based ILs with neutral or acidic anions, which is consistent with the base-catalysis of the exchange reaction previously observed in dilute aqueous solutions of 1,3-alkylimidazoliums, and previous reports of pH dependent exchange behavior in bmim BF_4. The exchange rate does not show a simple second-order dependence on the concentration of the reactants, but may be consistent with a base-catalyzed exchange mechanism if the increase in exchange rate at 0.43 mole fraction water is considered anomalous. The activities of the reactants and the concentrations of the potential intermediates are mediated by a complex interplay between non-covalent interactions and acid-base equilibria at different mole fractions of water.

Acknowledgements

The authors would like to acknowledge Dr. James Mao, who contributed the bond lengths for emim acetate. This technical effort was performed in support of the National Energy Technology Laboratory's (US-Department of Energy) ongoing research in CO_2 capture under the RES contract DE-FE0004000.

Notes and references

[a] *Department of Chemistry, University of Pittsburgh, Pittsburgh,15260 USA. Fax: 412-624-8611; Tel: 412-624-8403; E-mail: damodak@pitt.edu*

† Electronic Supplementary Information (ESI) available: [Rotational Correlation time calculations, proton spin-spin relaxation rates, EXSY diagonal and cross-peak volumes and NMR pulse sequence information are available in the supplementary information]. See DOI: 10.1039/b000000x/

1. J. S. Wilkes, *Green Chemistry*, 2002, **4**, 73-80.
2. S. Chowdhury, R. S. Mohan and J. L. Scott, *Tetrahedron*, 2007, **63**, 2363-2389.
3. M. B. Shiflett and A. Yokozeki, *Journal of Chemical & Engineering Data*, 2008, **54**, 108-114.
4. J. Vitz, T. Erdmenger, C. Haensch and U. S. Schubert, *Green Chemistry*, 2009, **11**, 417-424.
5. T. Heinze, S. Dorn, M. Schoebitz, T. Liebert, S. Koehler and F. Meister, *Macromol. Symp.*, 2008, **262**, 8-22.
6. M. Besnard, M. I. Cabaco, F. V. Chavez, N. Pinaud, P. J. Sebastiao, J. A. P. Coutinho and Y. Danten, *Chemical Communications*, 2012, **48**, 1245-1247.
7. M. Besnard, M. I. Cabaço, F. Vaca Chávez, N. Pinaud, P. J. Sebastião, J. A. P. Coutinho, J. Mascetti and Y. Danten, *The Journal of Physical Chemistry A*, 2012, **116**, 4890-4901.
8. M. Besnard, M. I. Cabaco, F. Vaca Chavez, N. Pinaud, P. J. Sebastiao, J. A. Coutinho, J. Mascetti and Y. Danten, *The journal of physical chemistry. A*, 2012, **116**, 4890-4901.
9. J. Blath, N. Deubler, T. Hirth and T. Schiestel, *Chemical Engineering Journal*, 2012, **181–182**, 152-158.
10. S. V. Troshenkova, E. S. Sashina, N. P. Novoselov, K. F. Arndt and S. Jankowsky, *Russ J Gen Chem*, 2010, **80**, 106-111.
11. C. A. Hall, K. A. Le, C. Rudaz, A. Radhi, C. S. Lovell, R. A. Damion, T. Budtova and M. E. Ries, *The journal of physical chemistry. B*, 2012, **116**, 12810-12818.
12. S. Fendt, S. Padmanabhan, H. W. Blanch and J. M. Prausnitz, *Journal of Chemical & Engineering Data*, 2010, **56**, 31-34.
13. C. A. Ober and R. B. Gupta, *Industrial & Engineering Chemistry Research*, 2012, **51**, 2524-2530.
14. K. Le, R. Sescousse and T. Budtova, *Cellulose*, 2012, **19**, 45-54.
15. W. Shi, K. Damodaran, H. B. Nulwala and D. R. Luebke, *Physical chemistry chemical physics : PCCP*, 2012, **14**, 15897-15908.
16. J. Kowalewski and L. Maler, in *Nuclear Spin Relaxation in Liquids: Theory, Experiments, and Applications*, eds. J. H. Moore and N. D. Spencer, Taylor & Francis, New York London, 2006, pp. 19-39; 195-197.
17. J. J. Allen, Y. Schneider, B. W. Kail, D. R. Luebke, H. Nulwala and K. Damodaran, *The Journal of Physical Chemistry B*, 2013, **117**, 3877-3883.
18. J. H. Antony, D. Mertens, A. Dolle, P. Wasserscheid and W. R. Carper, *Chemphyschem : a European journal of chemical physics and physical chemistry*, 2003, **4**, 588-594.
19. W. R. Carper, P. G. Wahlbeck, N. E. Heimer and J. S. Wilkes, in *Ionic Liquids IV*, eds. J. F. Brennecke, R. D. Rogers and K. R. Seddon, American Chemical Society, 2007, vol. 975, pp. 21-34.
20. W. R. Carper, P. G. Wahlbeck and A. Dölle, *The Journal of Physical Chemistry A*, 2004, **108**, 6096-6099.
21. W. R. Carper, *Concepts in Magnetic Resonance*, 1999, **11**, 51-60.
22. J. H. Antony, A. Dolle, D. Mertens, P. Wasserscheid, W. R. Carper and P. G. Wahlbeck, *Journal of Chemical Physics*, 2005, 6676-6682.
23. R. B. Buxton, *Introduction to Functional Magnetic Resonance Imaging : Principles and Techniques*, Cambridge University Press, Cambridge, UK; New York, 2002.
24. C. L. Perrin and T. J. Dwyer, *Chemical Reviews*, 1990, **90**, 935-967.
25. Y.-J. Kim and A. Streitwieser, *Journal of the American Chemical Society*, 2002, **124**, 5757-5761.
26. T. L. Amyes, S. T. Diver, J. P. Richard, F. M. Rivas and K. Toth, *Journal of the American Chemical Society*, 2004, **126**, 4366-4374.
27. S. T. Handy and M. Okello, *The Journal of Organic Chemistry*, 2005, **70**, 1915-1918.
28. R. A. Olofson, W. R. Thompson and J. S. Michelman, *Journal of the American Chemical Society*, 1964, **86**, 1865-1866.
29. R. W. Alder, P. R. Allen and S. J. Williams, *Journal of the Chemical Society, Chemical Communications*, 1995, **0**, 1267-1268.
30. Y. Yasaka, C. Wakai, N. Matubayasi and M. Nakahara, *The Journal of Physical Chemistry A*, 2007, **111**, 541-543.
31. Y. Zhao, S. Gao, J. Wang and J. Tang, *J. Phys. Chem. B*, 2008, **112**, 2031-2039.
32. H. Wennerstrom, B. Lindman, O. Soderman, T. drakenberg and J. B. Rosenholm, *Journal of the American Chemical Society*, 1979, **101**, 6860-6864.
33. N. V. Sastry, N. M. Vaghela, P. M. Macwan, S. S. Soni, V. K. Aswal and A. Gibaud, *Journal of Colloid and Interface Science*, 2012, **371**, 52-61.
34. W. S. Price and L.-P. Hwang, *Journal of the Chinese Chemical Society*, 1992, **39**, 479-496.
35. C. K. Larive, M. Lin, B. S. Kinnear, B. J. Piersma, C. E. Keller and W. R. Carper, *J. Phys. Chem. B*, 1998, **102**, 1717-1723.
36. S. Ohta, A. Shimizu, Y. Imai, H. Abe, N. Hatano and Y. Yoshimura, *Open J. Phys. Chem.*, 2011, **1**, 70-76.
37. Z. Zolnai, N. Juranić, D. Vikić-Topić and S. Macura, *Journal of Chemical Information and Computer Sciences*, 2000, **40**, 611-621.
38. O. Holloczki, D. Gerhard, K. Massone, L. Szarvas, B. Nemeth, T. Veszpremi and L. Nyulaszi, *New J. Chem.*, 2010, **34**, 3004-3009.